International Journal of
Intelligent Engineering & Systems

http://www.inass.org/

Epileptic Seizure Classification Based on Enhanced State Refinement Gated Recurrent Unit with Temporal Activation Regularization

Cholleti Sathyanarayana[1]* **Yerravelli Raghavender Rao[2]**

[1]*Department of Electronics and Communication Engineering,*
JNTUH and Sreenidhi Institute of Science and Technology, India
[2]*Department of Electronics and Communication Engineering, JNTUHUCES, India*
* Corresponding author's Email: sathyacholleti@gmail.com

Abstract: The neural activity in the brain is detected through Electroencephalography (EEG) which enables the analysis and classification of epileptic disorder. The epileptic classification is challenging due to the presence of noise and artifacts in the EEG signal which increases the False Positive Rate (FPR) and minimizes the classification performance. Therefore, this research proposes an Enhanced State Refinement Gated Recurrent Unit with Temporal Activation Regularization (ESRGRU-TAR) for epileptic seizure classification. The ESRGRU optimizes the gating mechanism to enhance the capability to capture long-term dependencies in the data. Particularly, refinements are capable of quality of interactive models that reveal interactions among sample points thereby enhancing interpretability. The message-passing mechanism is developed to highlight useful feature representations between sample points. TAR is beneficial for controlling overfitting because it moderates the model's activation by adding temporal consistency to the learning process. The BONN and CHB-MIT datasets are used to estimate the proposed ESRGRU-TAR performance based on the classifier. The ESRGRU-TAR achieves better accuracy of 99.91% and 99.89% for BONN and CHB-MIT datasets which is better than existing techniques such as Bidirectional Long Short-Term Memory (Bi-LSTM).

Keywords: Electroencephalography, Epileptic seizure classification, Enhanced state refinement gated recurrent unit, False positive rate, Temporal activation regularization.

1. Introduction

Epilepsy is a nervous disorder which affects around 1% of global population caused by the abnormal activity in group of nerve cells in the brain that resultant in epileptic seizures. Rapid changes in EEG signals are considered as a significant indicator in detection and classification of epileptic seizures [1]. The seizures in epileptic patients leads to severe clinical symptoms like abnormal behavior, loss of consciousness, muscle contractions, weird ambiences and so on [2]. Epileptic seizures are characterized by abnormal activities in brain which suffers from momentary and unnatural fluctuations in electrical activity [3]. Although most of the seizures are successfully managed using drug therapy, anti-epileptic medications and surgery give only partial relief and fail in 30% of the cases [4]. EEG gives instant information of the electrical output produced by nerve cells in the cerebral cortex which has great temporal resolution in the order of 10ms [5]. It also emerged that applying manual interventions to patients before the start of seizures greatly minimize patient anxiety, and positively influence the overall treatment process [6]. Hence, it is important to create a high precision epilepsy prediction by EEG to predict occurrence of seizure in patients [7, 8].

Early research on EEG signal analysis indicates that the signals generated by the brain are noisy and created from a chaotic dynamical system [9]. Determination of seizures in the epilepsy population is critical to correct diagnosis and developing personalized treatment strategies. This is because early diagnosis and regular follow-ups of seizure cases lead to better living quality and reduced lifethreatening complications [10, 11]. Recent research techniques for predicting seizures include time - frequency analysis, non-linear dynamics and Deep Learning (DL) networks [12]. While applying DL algorithms in different healthcare interventions, the same has also been incorporated in cloud-based seizure detection to enhance classification [13]. Many features are investigated via linear and non-linear techniques and integrated to characterize brain activity and dynamics for further higher dimensional analysis [14, 15]. The existing research uses DL algorithms like Convolutional Neural Networks (CNN) and Long Short-Term Memory (LSTM) for epileptic seizure classification. Generally, these algorithms were structured in a layered format, enabling the development of effective prediction models with less classification time for real-time applications [16, 17]. The research contributions are summarised as follows:

- The ESRGRU optimizes the gating mechanism to improve the capability of capturing long-term dependencies in data. The TAR is used to manage overfitting because it controls the model's activation by adding temporal consistency to the learning process.
- The integration of ESRGRU-TAR makes it possible to filter complex and noisy EEG data when increasing robustness against signal variation, which facilitates quicker generalization for various seizure patterns.
- Feature extraction techniques such as Short-Time Fourier Transform (STFT) and Discrete Wavelet Transform (DWT) capture temporal and frequency features of EEG signals which are used to distinguish seizure and non-seizures effectively.

This research paper is arranged as follows: Section 2 explains literature review, and Section 3 describes a proposed method in detail. Section 4 gives result analysis on BONN and CHB-MIT datasets. The conclusion of this research is provided in Section 5.

2. Literature review

Recently, DL algorithm have been extensively applied for epileptic seizure classification due to efficiency and its performance is analyzed in this section.

Zaid [18] suggested preprocessed and integrated EEG data for epileptic seizure classification by 1D-Convolution Neural Network original with Fast Fourier Transform (1D-CNN original + FFT). The preprocessed signals are given to the DL model but the EEG signals are combined into their original form. The 1D-CNN original + FFT method provided adequate prediction with a smaller number of nodes. Nevertheless, this only captured temporal information and did not suppose the rhythmic fluctuations of EEG signals which limits its discriminant ability to differentiate among seizure and non-seizure.

Jemal [19] introduced a CNN inspired by Filter Bank Common Spatial Pattern (FBCSP) for predicting epileptic seizures by EEG data. The CNN was interpretable due to the layer was visualized as result where learned weights flow from signal processing like spatial and sub-band filters. Subsequently, extracted features are no longer to commonly applied features for EEF data decoding. The CNN inspired by FBCSP achieved better performance in EEG predictions. However, hand-crafted features are extracted due to the limited representation capabilities which are not suitable for correctly classifying the EEG signals.

Voruganti and Gurrala [20] developed a Hierarchical LSTM (H-LSTM) with Skip Connection for epileptic seizure classification. The H-LSTM captures short and long-term dependence among nearest sequences for high-dimensional data. Skip connections are added between two consecutive H-LSTM layers to facilitate the data from one sequence to another for improving the classification accuracy of epileptic seizures. However, H-LSTM with skip connection has less temporal communication in subsequent sequence which lead to loss in important features required for accurate seizure classification.

Kumar [21] implemented a Bi-LSTM for epileptic seizure classification in EEG data. The Bi-LSTM reserves non-stationary nature of EEG data when minimizing processing costs through Local Mean Decomposition (LMD) and statistical feature extraction. A dual LSTM with an opposite propagation way was integrated which utilized data from before and after present time to determine output state. The Bi-LSTM effectively captured the long-term dependence both in forward and reverse direction on EEG signals. However, it did not suppose the rhythmic fluctuations of EEG signals which limits its discriminant ability to differentiate seizure and non-seizure patterns.

Daftari [22] presented a DL algorithm that involved two parallel processes of analyzing EEG signals for epileptic seizure activity. Time-frequency images of EEG data and raw waveforms were mandatory input features for CNN and RNN-LSTM.

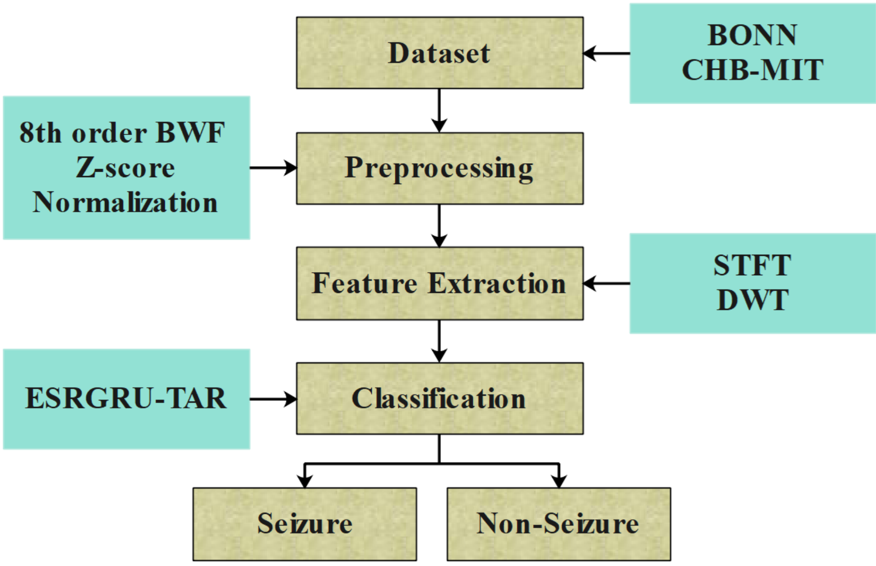

Figure. 1 Process of the proposed methodology

The spectrogram and scalogram image processing were developed using two signal processing methods such as STFT and CWT. However, the PCNN-LSTM has challenges in capturing high dimensional data between the consecutive sequences which affects the classifier performance.

From the above analysis, various issues are addressed in existing approaches such as the problem of modelling high dimensional features between adjacent sequences, high classification error rate due to concentration only on time-based features, weak flow of information across sequences and dependency on handcrafted features. To overcome these issues, this research proposes an ESRGRU-TAR to enhance capability to capture long-term dependencies in data. Moreover, STFT and DWT are to capture temporal and frequency features of EEG signals which are used to distinguish seizure and non-seizures effectively.

3. Proposed methodology

This research proposed an ESRGRU-TAR for epileptic seizure classification. Initially, BONN and CHB-MIT datasets are considered in this research, which is preprocessed by 8th order BWF filter and z-score normalisation to remove noise and normalise the data. Then, the preprocessed data is fed as input into the STFT and DWT to extract features from time and frequency domains. Fig. 1 denotes the process of epileptic seizure.

3.1 Dataset

Two widely accessible EEG datasets such as BONN [23] and CHB-MIT [24] are utilized in epileptic seizure prediction. A brief description of these datasets is given as follows:

3.1.1. BONN dataset

The BONN dataset contains five subsets, that are labelled as A, B, C, D and E. Each subset has a signal channel of EEG data by precise characteristics. The A and B subsets have scalp EEG data from healthy volunteers and subsets, whereas C and D subsets have intracranial EEG data from focal and non-focal patients. Lastly, the E subset has appropriate intracranial EEG signals. Every subset has 100 files, in which every file has 4096 samples with a recording of 23.6s and a sampling rate of 173.61Hz.

3.1.2. CHB-MIT dataset

The CHB-MIT dataset is gathered from Boston Children's Hospital, which includes data attained from interictal and seizure periods with 10-20 international standard electrode placement system. This dataset has numerous channels of EEG records by 256Hz sample rate and 23 records from 22 subjects.

3.2 Preprocessing

The EEG signal is preprocessed for attaining significant features with higher possibilities of interictal and ictal correlation portions. The preprocessed techniques such as 8th order BWF and z-score normalization are used in this research.

3.2.1. 8^{th} order Butter worth filter

The EEG signals are preprocessed at 60Hz frequency using 8th order BWF to remove two types of irrelevant noises such as mechanical and electrical [25]. The highest-order filter is applied because of its ability to gain bandwidth. The continuous value of 8th order BWF is calculated by Eq. (1).

$$G^2(W) = \frac{G_0^2}{1+\left(\frac{jw}{jw_c}\right)^{2n}} \quad (1)$$

Where, the direct present gain is presented through G_0, the cut-off frequency is provided through w_c and filter order is n.

3.2.2. Z-score normalization

Normalization is performed by dual signals for predefined or same series [20]. The predefined series samples are statistical discernment of normalization that converts signal where mean and standard deviations are 1. The Z-score normalization is performed for normalization which exposes classification performance through signal flattening. The mathematical expression of the z-score value is provided in Eq. (2).

$$z - score = \frac{score - mean}{standard\ deviation} \quad (2)$$

The $score$ is the data point, the $mean$ is the average of every data point and $standard\ deviation$ is the number of data variations. The normalization process preserves the correlation among actual and normalized EEG signals which minimizes the bias selection. The z-score normalization standardizes EEG data and improves discriminative features.

3.3 Feature Extraction

The preprocessed signals are provided as input to feature extraction to extract time and frequency features. The STFT and DWT are used in this research to extract time and frequency domains.

3.3.1. Short-Time Frequency Transform (STFT)

The STFT extracts a representation of time-frequency in EEG signals which provide important features for epileptic seizure classification [20]. The time-frequency features capture spectral variations over a short period and generate discriminative features that differentiate between seizure and non-seizure. In STFT, non-stationary signals are separated into small segments and those segments are taken as sequential. These portions are attained by windowing function and this technique is known as windowing signals. The time-dependent signals are stated in time and frequency axes by using the STFT method. The STFT ($\gamma(w,\tau)$) is numerically provided in Eq. (3).

$$\gamma(w,\tau) = STFT\{f(t)\} = \int f(t)W(t - \tau)e^{-jwt}\,dt \quad (3)$$

Here, $f(t), W, w$ and t are time domain signal, windowing function, frequency parameters and time parameter. The $\gamma(w,\tau)$ is a result of SIFT, e^{-jwt} is an exponential function and τ is a slow time parameter. Here, the hamming is applied as a windowing function in STFT. For BONN and CHB-MIT datasets, the window size is determined as 4128.64 and its parameter has some points for overlapping between windows which is utilized and decided 2,64,32.

3.3.2. Discrete Wavelet Transform (DWT)

The spectral analysis is used for analyzing non-stationary signs and transforms them into time-frequency domain. The DWT decomposes a signal into a group of sub-bands named as a coefficient approximation $A_i(k)$ and coefficient detail $D_i(k)$ through high and low-pass filters respectively. The $A_i(k)$ and $D_i(k)$ in ith level is defined in Eq. (4) and (5).

$$A_i = \left\{\frac{1}{\sqrt{M}}\sum_x f(x)\cdot\varphi_{j,k}(x)\right\} \quad (4)$$

$$D_i = \left\{\frac{1}{\sqrt{M}}\sum_x f(x)\cdot\psi_{j,k}(x)\right\} \quad (5)$$

Where, high-pass filter is named as g respective to discrete function $\varphi_{j,k}(x)$ as shown in the Eq. (6) and low-pass filter named as h is minor version using scaling function $\varphi_{j,k}(x)$ as shown in Eq. (7).

$$\varphi_{j,k}(x) = 2^{j/2}h\left(\left(2^j x - k\right)\right) \quad (6)$$

$$\psi_{j,k}(x) = 2^{j/2}g\left(\left(2^j x - k\right)\right) \quad (7)$$

The DWT is efficient in capturing both time and frequency information which enables for isolation of relevant features related to seizures thereby enhancing classification performance.

3.4 Classification

The ESRGRU is developed in this research which leverages temporal interaction data among signal points in EEG signals. The traditional GRU gathers the input sample points individually without taking

Received: November 30, 2024. Revised: December 17, 2024.

interactions among them. For signal point i, presentations of tth step is embedded as vector form $e_t^i = \phi_e(x_t^i, y_t^i; W_e)$, where, ϕ_e is an embedding function which is parameterized by W_e, e_t^i is applied as input to GRU as Eqs. (8)- (11).

$$g_{z,t}^i = \sigma\left(W^z e_t^i + U^z h_{t-1}^i + b^z\right) \tag{8}$$

$$g_{u,t}^i = \sigma\left(W^u e_t^i + U^u h_{t-1}^i + b^u\right) \tag{9}$$

$$C_t^i = tanh\left(W^C e_t^i + U^C g_{u,t}^i h_{t-1}^i + b^C\right) \tag{10}$$

$$H_t^i = (1 - g_{z,t}^i) \cdot H_{t-1}^i + g_{z,t}^i \cdot C_t^i \tag{11}$$

Where, g is a GRU gate function and its respective superscripts such as z and u are reset and update gate. C_t^i and H_t^i are unit and hidden state of GRU, W and U are respective weight matrices. Particularly, each sample point is taken as an individual object when applying the GRU with all parameters transformed among sample points. Based on derivative of hidden state H_t^i from GRU, states at sample point $i + 1$ are directly determined using Eq. (12).

$$\left[x_t^{i+1}, y_t^{i+1}\right]^T = W_d H_t^i \tag{12}$$

Where, W_d is a learned hyperparameters through reducing loss function. During inference phase, earlier space state is applied as inputs to the present space step. The traditional GRU is applied to extract features from the meaningful representation of every sample point individually. The ESRGRU is applied to improve unit states C_t^i through passing messages among sample points in EEG. The ESRGRU has three information sources for all sample points as inputs such as present representation of sample points, hidden state and unit state of GRU. The result of ESRGRU are refined unit states and its numerical formula is provided in Eq. (13).

$$\hat{C}_t^{i,l+1} = \sum_{k\in T(t)} G_k\left(\hat{H}_k^{i,l}, \hat{H}_t^{i,l}\right) + \hat{C}_t^{i,l} \tag{13}$$

Where, G is a message passing function and $T(t)$ is an EEG sample episode of T length. At step t, hidden state $\hat{H}_k^{i,l}$ from adjacent sample point with $k \in T(t)$ are combined through passing function and integrated by unit state of t for obtaining refined unit states. The message-passing process is achieved for various iterations and l is a message passing iteration index. After $l = 0$, states are adjusted through traditional GRU in Eqs. (8)- (11). Second, the unit state is refined through L alteration iterations in the ESRGRU module and utilized for deriving subsequent states as Eqs. (14)- (16).

$$\hat{C}_t^i = C_t^{i,L} \tag{14}$$

$$\hat{H}_t^i = g_{u,t}^i \cdot tanh\,(\hat{C}_t^i) \tag{15}$$

$$\left[x_t^{i+1}, y_t^{i+1}\right]^T = W_d \hat{H}_t^i \tag{16}$$

Where, $g_{u,t}^i$ is derivative from traditional GRU. Particularly, refinements are proficient quality of interactive model which revealing interactions among sample points thereby enhancing interpretability. To adaptively select valuable feature representation from adjacent sample points and allow message passing, this research introduces a message passing term G by-feature representation screening framework as Eq. (17).

$$\hat{C}_t^{i,l+1} = \begin{cases} \sum_{k\in T(t)} G_k\left(\hat{H}_k^{i,l}, \hat{H}_t^{i,l}\right) + \hat{C}_t^{i,l} \\ \sum_{k\in T(t)} W^{md}\, \alpha_{t,k}^{i,l} \cdot \left(g_{t,k}^{m,i,l} \odot \hat{H}_k^{i,l}\right) + \hat{C}_t^{i,l} \end{cases} \tag{17}$$

Where, $\odot, W^{md}, \alpha_{t,k}$ and $g_{t,k}$ are element-wise product, transform parameters, sample point-wise attention and gate representation respectively. The $\alpha_{t,k}$ is a scalar and this attention for sample point with $k \in T(t)$ is determined by Eqs. (18) and (19).

$$u_{t,k}^{i,l} = W^{\alpha^T}\left[r_{t,k}^{i,l}; \hat{h}_k^{i,l}; \hat{h}_t^{i,l}\right] \tag{18}$$

$$\alpha_{t,k}^{i,l} = \frac{\exp\left(u_{t,k}^{i,l}\right)}{\sum_d u_{t,d}^{i,l}} \tag{19}$$

Where, $r_{t,k}^{i,l}$ is a relative temporal state for empowering feature information screening which is embedded through its function $\emptyset_r$ as Eq. (20).

$$r_{t,k}^{i,l} = \emptyset_r\left(x_t^i - x_k^i, y_t^i - y_k^i; W^r\right) \tag{20}$$

Where, $\left(x_t^i, y_t^i\right)$ is a sample point representation i at step t, similarly for $\left(x_k^i, y_k^i\right)$ and W^r is a parameter for $\emptyset_r$. The $g_{t,k}$ is a vector and it is determined using Eq. (21).

$$g_{t,k}^{m,i,l} = \sigma\left(W^m\left[r_{t,k}^{i,l}; \hat{h}_k^{i,l}; \hat{h}_t^{i,l}\right] + b^m\right) \tag{21}$$

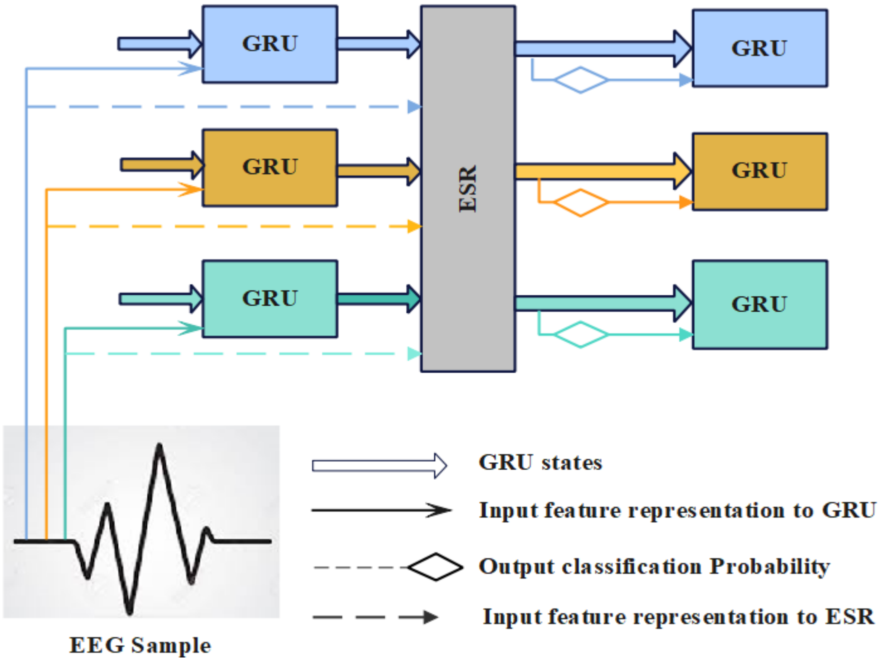

Figure. 2 Architecture of ESRGRU

Where, $g_{t,k}^{m}$ is a feature screening, σ is a sigmoid function, W^{m} and b^{m} are respective parameters. It is required to recognize that the representation gate and signal point-wise attention operate in parallel to filter feature information from adjacent signal points which allows effective message exchange. The representation gate based on the following integration $r_{t,k}^{i}, \hat{h}_{k}^{i}$ and $\hat{h}_{t}^{i}$ which implements on every hidden state $\hat{h}_{k}^{i}$ to execute a pairwise feature screening thus it guarantees that current signal points have corresponding feature representations of sample point t and k and their relative temporal and their corresponding relative time, for feature screening are detected and combined simultaneously. Fig. 2 depicts the architecture of ESRGRU.

However, sample point-wise attention enhances the dependencies among strongly related signal points and controls the exchange of intermediary messages between neighbouring nodes. To prevent any overshooting during imputation, the TAR is applied to the consecutive hidden layers. This regularization quantifies the sum of all the loss terms mathematically equal to the difference between the final and initial hidden layers. A small weight is assigned to this loss to ensure that the imputation results are still different over time. Thus, a weight value α of 0.0001 is empirically selected as Eq. (22).

$$l_{temporal\_reg} = \alpha L_2(h_t, h_{t-1}) \tag{22}$$

The ESRGRU is uses a gating mechanism to enhance capability for capturing long-term dependencies when dealing with EEG signals with varying temporal structures. The TAR is beneficial to control overfitting because it moderates model's activation by including temporal consistency in the learning process. The integration of ESRGRU-TAR makes it possible to filter complex and noisy EEG data when increasing robustness against signal variation which enables quicker generalization for several seizure patterns.

4. Experimental results

The ESRGRU-TAR is simulated in MATLAB software with system requirements of 6GB RAM, windows 10 OS and Intel i5 processor. The accuracy, specificity, precision, f1-score, sensitivity, AUC and FPR are taken as metrics to evaluate ESRGRU-TAR performance for BONN and CHB-MIT datasets. The mathematical representation for all these metrics is provided in Eqs. (23)- (29).

$$Accuracy = \frac{TP+TN}{TP+TN+FP+FN} \tag{23}$$

$$Specificity = \frac{TN}{TN+FP} \tag{24}$$

$$Precision = \frac{TP}{TP+FP} \tag{25}$$

$$F1-score = 2 \times \frac{Precision \times Sensitivity}{Precision+Sensitivity} \tag{26}$$

 DOI: 10.22266/ijies2025.0229.83

Received: November 30, 2024. Revised: December 17, 2024.

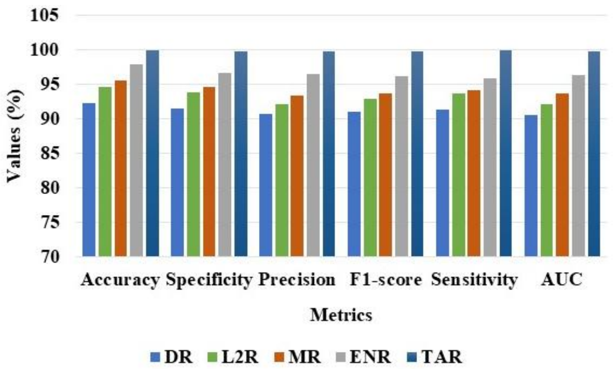

Figure. 3 TAR performance for BONN dataset

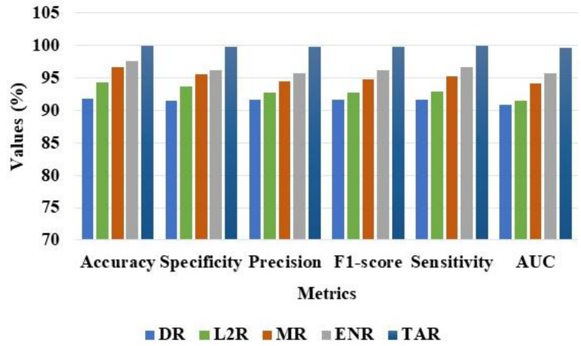

Figure. 4 TAR performance for CHB-MIT dataset

Table 1. ESRGRU-TAR performance for BONN dataset

Method	Accuracy (%)	Specificity (%)	Precision (%)	F1-score (%)	Sensitivity (%)	AUC (%)	FPR (%)
CNN	90.62	89.79	88.81	89.20	89.61	90.48	-88.79
RNN	93.73	91.66	90.34	90.94	91.55	91.28	-90.66
LSTM	94.71	93.47	92.52	92.98	93.46	94.67	-92.47
GRU	96.58	95.75	95.56	95.11	94.68	95.62	-94.75
ESRGRU-TAR	99.91	99.83	99.87	99.88	99.90	99.79	-98.83

$$Sensitivity = \frac{TP}{TP+FN} \tag{27}$$

$$AUC = \frac{\sum R_i(I_I) - I_I(I_I+I)/2}{I_I+I_f} \times 100 \tag{28}$$

$$FPR = 1 - specificity \tag{29}$$

Where, TP, TN, FP and FN are True Positive, True Negative, False Positive and False Negative respectively. The R_i is a ith signal point, I_I and I_f are the initial and final points of signal interval respectively.

Fig. 3 indicates the TAR performance for BONN dataset with metrics of accuracy, specificity, precision, f1-score, sensitivity and AUC. The state-of-art methods like Dropout Regularization (DR), L2 Regularization (L2R), Max-norm Regularization (MR) and Elastic Net Regularization (ENR) are taken to compare the TAR performance. The TAR achieves accuracy 99.91%, specificity 99.83%, precision 99.87%, f1-score 99.88%, sensitivity of 99.90% and AUC 99.79% for BONN dataset.

Table 1 indicates the ESRGRU-TAR performance for BONN dataset with metrics of accuracy, specificity, precision, f1-score, sensitivity, AUC and FPR. State-of-the-art methods like Convolution Neural Network (CNN), Recurrent Neural Network (RNN), Long Short-Term Memory (LSTM) and GRU are used to compare the ESRGRU-TAR performance. The ESRGRU-TAR achieves accuracy of 99.91%, specificity of 99.83%, precision of 99.87%, f1-score of 99.88%, sensitivity of 99.90%, AUC of 99.79% and FPR of -98.83% for BONN dataset.

Fig. 4 indicates the TAR performance for CHB-MIT dataset with metrics of accuracy, specificity, precision, f1-score, sensitivity, and AUC. State-of-the-art methods like DR, L2R, MR, and ENR are used to compare the TAR performance. The TAR achieves accuracy of 99.89%, specificity of 99.82%, precision of 99.78%, f1-score of 99.82%, sensitivity of 99.88%, and AUC of 99.67% for the CHB-MIT dataset.

Table 2 indicates ESRGRU-TAR performance for the BONN dataset with metrics of accuracy, specificity, precision, f1-score, sensitivity, AUC and FPR. State-of-the-art methods like CNN, RNN, LSTM, and GRU are used to compare the ESRGRU-TAR performance. The ESRGRU-TAR achieves accuracy of 99.89%, specificity of 99.82%, precision 99.78%, f1-score 99.82%, sensitivity of 99.88%, AUC of 99.67% and FPR -98.82% for CHB-MIT dataset. The Fig. 5 and Fig. 6 shows the confusion matrix for BONN and CHB-MIT dataset respectively. The Fig. 7 and Fig. 8 shows the ROC-AUC curve for BONN and CHB-MIT datasets respectively.

4.1 Comparative analysis

The comparison of ESRGRU-TAR is provided in this section with metrics of accuracy, specificity, precision, f1-score, sensitivity and AUC for BONN and CHB-MIT datasets.

Received: November 30, 2024. Revised: December 17, 2024.

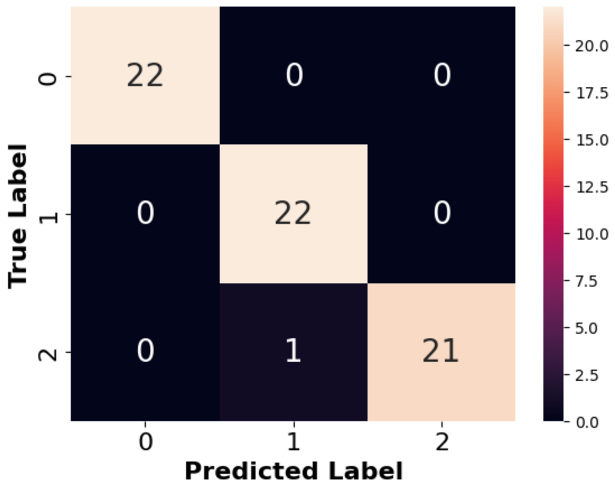

Figure. 5 Confusion matrix for BONN dataset

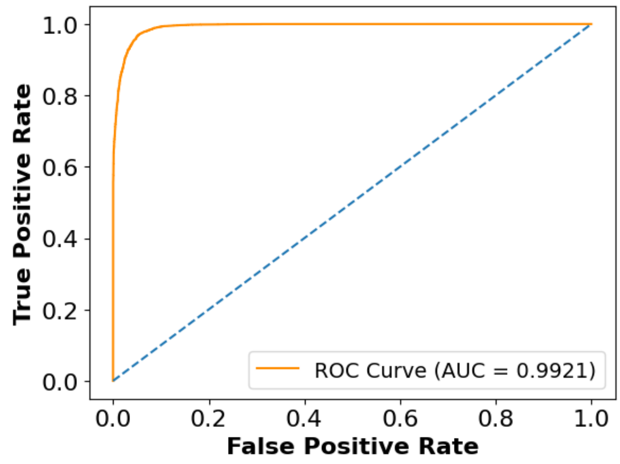

Figure. 7 ROC-AUC curve for BONN dataset

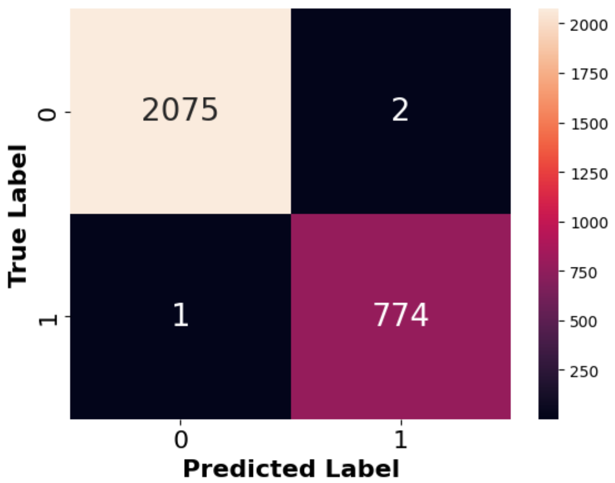

Figure. 6 Confusion matrix for CHB-MIT dataset

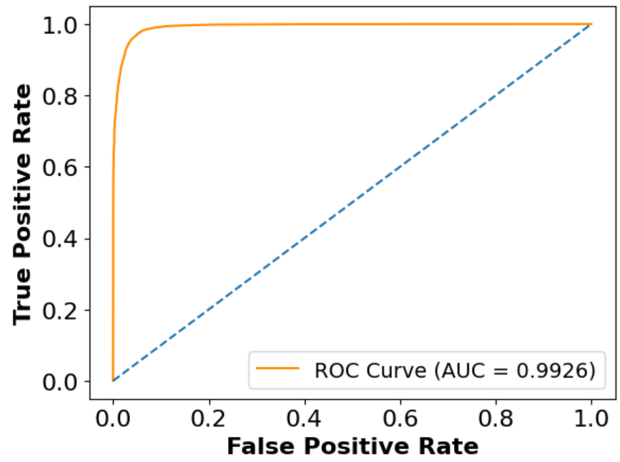

Figure. 8 ROC-AUC curve for CHB-MIT dataset

Table 2. ESRGRU-TAR performance for the CHB-MIT dataset

Method	Accuracy (%)	Specificity (%)	Precision (%)	F1-score (%)	Sensitivity (%)	AUC (%)	FPR (%)
CNN	92.56	91.74	91.62	91.16	90.71	91.51	-90.74
RNN	94.54	94.36	93.58	93.10	92.64	94.13	-93.36
LSTM	95.77	95.15	94.41	94.48	94.57	95.65	-94.15
GRU	97.18	96.57	95.50	95.43	95.38	95.48	-95.57
ESRGRU-TAR	99.89	99.82	99.78	99.82	99.88	99.67	-98.82

Table 3. Comparison of ESRGRU-TAR for BONN dataset

Method	Accuracy (%)	Specificity (%)	F1-score (%)	Sensitivity (%)	AUC (%)
1D-CNN original + FFT [18]	99.13	99.34	NA	98.32	NA
H-LSTM with skip connection [20]	99.81	99.75	99.79	99.87	NA
PCNN-LSTM [22]	99.75	99.62	99.83	99.83	99.56
ESRGRU-TAR	99.91	99.83	99.88	99.90	99.79

Table 4. Comparison of ESRGRU-TAR for CHB-MIT dataset

Method	Accuracy (%)	Specificity (%)	Precision (%)	F1-score (%)	Sensitivity (%)	AUC (%)
CNN inspired by FBCSP [19]	90.9	84.7	88.5	91.9	96.1	91.8
H-LSTM with skip connection [20]	99.34	99.62	NA	99.54	99.86	NA
Bi-LSTM [21]	97.00	93.90	NA	NA	95.70	NA
PCNN-LSTM [22]	97.12	97.49	NA	97.27	96.75	96.72
ESRGRU-TAR	99.89	99.82	99.78	99.82	99.88	99.67

The ESRGRU-TAR performance is compared with 1D-CNN original + FFT [18], CNN inspired by FBCSP [19], H-LSTM with skip connection [20], Bi-LSTM [21] and PCNN-LSTM [22] to show the effectiveness. The ESRGRU-TAR achieves accuracy of 99.91%, specificity 99.83%, precision of 99.87%, f1-score of 99.88%, sensitivity of 99.90% and AUC of 99.79% for BONN dataset. The ESRGRU-TAR achieves accuracy 99.89%, specificity 99.82%, precision 99.78%, f1-score 99.82%, sensitivity 99.88% and AUC 99.67% for the CHB-MIT dataset. Table 3 and Table 4 indicate the comparison of ESRGRU-TAR for BONN and CHB-MIT datasets respectively.

4.2 Discussion

The section describes the results achieved from ESRGRU-TAR for improving classification performance of epileptic seizures. The 1D-CNN original + FFT [18] only captured temporal information and did not suppose the rhythmic fluctuations of EEG signals which limits its discriminant ability in differentiate among seizure and non-seizure. In CNN inspired by FBCSP [19], handcrafted features are extracted due to the limited representation capabilities which are not suitable for accurately classifying EEG signals. The H-LSTM with skip connection [20] has reduced temporal communication in subsequent sequences which leads to loss of important features required for accurate seizure classification. The Bi-LSTM [21] did not suppose the rhythmic fluctuations of EEG signals which limits its discriminant ability to differentiate among seizure and non-seizure. PCNN-LSTM [22] has challenges in capturing high dimensional data between consecutive sequences which affect the classifier performance. To overcome this drawback, the ESRGRU-TAR is proposed in this research which enhances the capacity to capture diverse temporal structures in EEG which are significance in accurate seizure classification. The TAR is used to manage overfitting because it controls the model's activation by adding temporal consistency to learning process. The integration of ESRGRU-TAR makes it possible to filter complex and noisy EEG data when increasing robustness against signal variation which facilitates quicker generalization for various seizure patterns.

5. Conclusion

This research proposes an ESRGRU-TAR based classification for epileptic seizure which makes it possible to filter complex and noisy EEG data when improving robustness against signal variation. The ESRGRU optimizes the gating mechanism to enhance capability for capturing long-term dependencies in data. The state refinements are proficient for interactive model quality which exposes interactions among sample points thereby improving interpretability. The 8th order BWF filter and z-score normalization are considered preprocessing to remove noise and normalize the EEG data. Feature extraction techniques such as STFT and DWT capture temporal and frequency features of EEG signals which are used to distinguish seizure and non-seizures effectively. The ESRGRU-TAR attains optimal accuracy of 99.91% and 99.89% for BONN and CHB-MIT datasets which is better than existing techniques. In future, optimization-based feature selection can be used to remove irrelevant features to further enhance the classification performance.

Notation list

Notations	Description
G_0	Direct present gain
w_c	Cut-off frequency
n	Filter order
$f(t)$	Time domain signal
W	Windowing function
w	Frequency parameters
t	Time parameter
$\gamma(w,\tau)$	Result of SIFT
e^{-jwt}	Exponential function
τ	Slow time parameter
$A_i(k)$	Coefficient approximation
$D_i(k)$	Coefficient detail

g	High-pass filter
$\varphi_{j,k}(x)$	Discrete function
h	Low-pass filter
$\varphi_{j,k}(x)$	Scaling function
i	Signal point
ϕ_e	Embedding function
W and U	Weight matrices
z and u	Reset and update gate
C_t^i and H_t^i	Unit and hidden state
W_d	Learned hyperparameters
G	Message passing function
$T(t)$	EEG sample episode of T length
l	Message passing iteration index
L	Alteration iterations
$\odot$	Element-wise product
W^{md}	Transform parameters
$\alpha_{t,k}$	Sample point-wise attention
$g_{t,k}$	Gate representation
$\alpha_{t,k}$	Scalar
$r_{t,k}^{i,l}$	Relative temporal state
(x_t^i, y_t^i)	Sample point representation
$g_{t,k}^m$	Feature screening
σ	Sigmoid function
W^m and b^m	Parameters
TP	True Positive
TN	True Negative
FP	False Positive
FN	False Negative
R_i	Signal point
I_I and I_f	Initial and final points

Conflicts of Interest

The authors declare no conflict of interest.

Author Contributions

The paper conceptualization, methodology, software, validation, formal analysis, investigation, resources, data curation, writing—original draft preparation, writing—review and editing, visualization, have been done by 1st author. The supervision and project administration, have been done by 2nd author.

References

[1] E. Tuncer, and E.D. Bolat, "Classification of epileptic seizures from electroencephalogram (EEG) data using bidirectional short-term memory (Bi-LSTM) network architecture", *Biomedical Signal Processing and Control*, Vol. 73, p. 103462, 2022.

[2] K. Singh, and J. Malhotra, "Predicting epileptic seizures from EEG spectral band features using convolutional neural network", *Wireless Personal Communications*, Vol. 125, No. 3, pp. 2667-2684, 2022.

[3] I. Ahmad, X. Wang, D. Javeed, P. Kumar, O.W. Samuel, and S. Chen, "A hybrid deep learning approach for epileptic seizure detection in EEG signals", *IEEE Journal of Biomedical and Health Informatics*, 2023.

[4] I. Assali, A.G. Blaiech, A.B. Abdallah, K.B. Khalifa, M. Carrère, and M.H. Bedoui, "CNN-based classification of epileptic states for seizure prediction using combined temporal and spectral features", *Biomedical Signal Processing and Control*, Vol. 82, p. 104519, 2023.

[5] O. Ouichka, A. Echtioui, and H. Hamam, "Deep learning models for predicting epileptic seizures using iEEG signals", *Electronics*, Vol. 11, No. 4, p. 605, 2022.

[6] W. Hu, J. Cao, X. Lai, and J. Liu, "Mean amplitude spectrum based epileptic state classification for seizure prediction using convolutional neural networks", *Journal of Ambient Intelligence and Humanized Computing*, Vol. 14, No. 11, pp. 15485-15495, 2023.

[7] C. Li, Z. Deng, R. Song, X. Liu, R. Qian, and X. Chen, "EEG-based seizure prediction via model uncertainty learning", *IEEE Transactions on Neural Systems and Rehabilitation Engineering*, Vol. 31, pp. 180-191, 2023.

[8] M. Varlı, and H. Yılmaz, "Multiple classification of EEG signals and epileptic seizure diagnosis with combined deep learning", *Journal of Computational Science*, Vol. 67, p. 101943, 2023.

[9] S. Ravi, S. Shreenidhi, A. Shahina, N. Ilakiyaselvan, and A.N. Khan, "Epileptic seizure detection using convolutional neural networks and recurrence plots of EEG signals", *Multimedia Tools and Applications*, Vol. 81, No. 5, pp. 6585-6598, 2022.

[10] H. Kode, K. Elleithy, and L. Almazedah, "Epileptic Seizure detection in EEG signals using Machine Learning and Deep Learning Techniques", *IEEE Access*, vol. 12, pp. 80657-80668, 2024.

[11] R.I. Halawa, S.M. Youssef, and M.N. Elagamy, "An efficient hybrid model for patient-independent seizure prediction using Deep Learning", *Applied Sciences*, Vol. 12, No. 11, p. 5516, 2022.

[12] X. Wu, T. Zhang, L. Zhang, and L. Qiao, "Epileptic seizure prediction using successive variational mode decomposition and transformers deep learning network", *Frontiers in Neuroscience*, Vol. 16, p. 982541, 2022.

[13] K. Singh, and J. Malhotra, “Smart neurocare approach for detection of epileptic seizures using deep learning based temporal analysis of EEG patterns”, *Multimedia Tools and Applications*, Vol. 81, No. 20, pp. 29555-29586, 2022.

[14] B. Jaishankar, A.M. Ashwini, D. Vidyabharathi, and L. Raja, “A novel epilepsy seizure prediction model using deep learning and classification”, *Healthcare Analytics*, Vol. 4, p. 100222, 2023.

[15] S. Mekruksavanich, and A. Jitpattanakul, “Effective Detection of Epileptic Seizures through EEG Signals Using Deep Learning Approaches”, *Machine Learning and Knowledge Extraction*, Vol. 5, No. 4, pp. 1937-1952, 2023.

[16] F.E. Ibrahim, H.M. Emara, W. El-Shafai, M. Elwekeil, M. Rihan, I.M. Eldokany, T.E. Taha, A.S. El-Fishawy, E.S.M. El-Rabaie, E. Abdellatef, and F.E.A. El-Samie, “Deep-learning-based seizure detection and prediction from electroencephalography signals”, *International Journal for Numerical Methods in Biomedical Engineering*, Vol. 38, No. 6, p. e3573, 2022.

[17] K. Singh, and J. Malhotra, “Prediction of epileptic seizures from spectral features of intracranial eeg recordings using deep learning approach”, *Multimedia Tools and Applications*, Vol. 81, No. 20, pp. 28875-28898, 2022.

[18] Y. Zaid, M. Sah, and C. Direkoglu, “Pre-processed and combined EEG data for epileptic seizure classification using deep learning”, *Biomedical Signal Processing and Control*, Vol. 84, p. 104738, 2023.

[19] I. Jemal, N. Mezghani, L. Abou-Abbas, and A. Mitiche, “An interpretable deep learning classifier for epileptic seizure prediction using EEG data”, *IEEE Access*, Vol. 10, pp. 60141-60150, 2022.

[20] N. Voruganti, and V.K. Gurrala, “Classification of Epileptic Seizure Using Hierarchical Long Short-Term Memory with Skip Connection Method”, *International Journal of Intelligent Engineering & Systems*, Vol. 17, No. 4, 970-980, 2024, doi: 10.22266/ijies2024.0831.73.

[21] P.R. Kumar, B. Shilpa, R.K. Jha, and S.N. Mohanty, “A novel end-to-end approach for epileptic seizure classification from scalp EEG data using deep learning technique”, *International Journal of Information Technology*, Vol. 15, No. 8, pp. 4223-4231, 2023.

[22] C. Daftari, J. Shah, and M. Shah, “Detection of epileptic seizure disorder using EEG signals”, In: *Artificial Intelligence-based Brain-Computer Interface*, pp. 163-188, 2022.

[23] BONN dataset link: https://www.upf.edu/web/ntsa/downloads/-/asset_publisher/xvT6E4pczrBw/content/2001-indications-of-nonlinear-deterministic-and-finite-dimensional-structures-in-time-series-of-brain-electrical-activity-dependence-on-recording-regi (accessed on October 2024).

[24] CHR-MIT dataset link: https://physionet.org/content/chbmit/1.0.0/ (accessed on October 2024).

[25] T.J. Rani, and D. Kavitha, “Classification of Epileptic Seizures Using LSTM Based Zebra Optimization Algorithm with Hyperparameter Tuning”, *International Journal of Intelligent Engineering & Systems*, Vol. 17, No. 3, pp. 80-91, 2024, doi: 10.22266/ijies2024.0630.07.